Poly(4-vinylpyridine)/$NiCo_2S_4$/polyaniline nanocomposites as supercapacitor electrode materials in alkaline media

Mohyaddin Gholizadeh Ghaleh-Aziz[1,2], Reza Najjar[1*], Mir Ghasem Hosseini[2]

[1]Polymer Research Laboratory, Faculty of Chemistry, University of Tabriz, Tabriz, Iran

[2]Electrochemistry Research Laboratory, Department of Physical Chemistry, Faculty of Chemistry, University of Tabriz, Tabriz, Iran.

Abstract

Nanocomposites composed of poly(4-vinylpyridine) (P4VPy), $NiCo_2S_4$ (NCS), and polyaniline (PAni) were synthesized and examined as promising electrode materials for supercapacitors. The hydrothermally prepared NCS formed a well-connected network structure, which contributed to an increased number of electroactive sites and improved charge transfer, leading to enhanced supercapacitor performance. The chemical characteristics of the nanocomposites were analyzed using FT-IR and EDX techniques, while their crystal structure and surface morphology were studied through XRD and FE-SEM, respectively. Electrochemical behavior was assessed using electrochemical impedance spectroscopy (EIS), galvanostatic charge–discharge (GCD), and cyclic voltammetry (CV). At a scan rate of 90 mV/s, the P4VPy/NCS/PAni nanocomposite demonstrated a specific capacitance of 347.3 F/g (from CV data). GCD analysis at a current density of 0.20 mA/g also showed that the nanocomposite had a capacitance of 95.82 F/g—nearly three times greater than that of pure P4VPy. This improvement is attributed to fast faradaic redox interactions between the conductive components and NCS, which created a strong synergistic effect, boosting energy storage capacity. These findings highlight the potential of heterogeneous nanomaterials in advancing energy storage technologies.

1.Introduction

Renewable energy sources require efficient electrical energy storage for use in everyday devices such as electric vehicles and smartphones [1, 2, 3]. Supercapacitors, compared to batteries, offer faster charge/discharge rates, flexibility, wide operating temperature, light weight, and simple maintenance [4, 5, 6]. Improving supercapacitor performance largely depends on developing high-performance electrode materials [7, 8, 9, 10]. Metal oxides (e.g., RuO_2, V_2O_5, MnO_2) [11] and mixed metal oxides have been widely studied for their fast redox reactions and multiple oxidation states [9, 12]. Recently, mixed metal sulfides like $NiCo_2S_4$ (NCS) have gained attention due to better electrochemical properties and conductivity [13]. Nanostructured metal sulfides show unique performances owing to their special crystal structures and rapid redox behavior. Conductive polymers such as polyaniline (PAni), with tunable conductivity and low cost, are promising for composite electrodes [14]. Their π-conjugated systems enhance charge transfer, especially when combined with metal oxides or sulfides [15]. Non-conductive polymers containing heteroatoms can also improve dispersion and conductivity of nanoparticles [16]. This study focuses on poly(4-vinylpyridine) (P4VPy), a polymer with nitrogen-containing side groups capable of coordinating with metal atoms, as a matrix to fabricate nanocomposites with NCS and PAni (P4VPy/NCS/PAni). The effect of incorporating hydrothermally synthesized NCS and PAni nanoparticles on supercapacitive performance is evaluated and compared to similar literature reports.

2.1 Materials

High purity grade nickel (II) nitrate ($Ni(NO_3)_2{\cdot}6H_2O$), cobalt (II) nitrate ($Co(NO_3)_2){\cdot}6H_2O$, potassium peroxydisulfate ($K_2S_2O_8$, KPS) and N-methylformamide (NMF) were obtained from Merck, Germany. Poly(2-vinylpyrrolidone) (P4VPy) and thioacetamide were from Sigma-Aldrich. Aniline (from Merck, Germany) was distillated under vacuum used as fresh for polymerization. Aniline was oxidatively polymerized by using KPS as oxidant/initiator in the hydrochloric acid (Merck) solution to obtain PAni. Urea was from Pardis Petrochemical Company, Iran. Deionized (DI) water was used in whole experiments.

2.2- Synthesis of $NiCo_2S_4$

Nickel cobalt sulfide ($NiCo_2S_4$, NCS) was prepared via a hydrothermal synthesis method. Initially, 1.454 g (5 mmol) of $Ni(NO_3)_2{\cdot}6H_2O$ and 2.91 g (16 mmol) of $Co(NO_3)_2{\cdot}6H_2O$ were dissolved in 30 ml of deionized (DI) water with magnetic stirring. Separately, a solution of 3 g (50 mmol) urea in 30 ml DI water was prepared and then added to the nickel and cobalt solution while stirring. Subsequently, 1.65 g (22 mmol) of thioacetamide was introduced to the mixture and stirred for 30 minutes. The resulting solution was transferred into an 80 ml Teflon-lined autoclave, which was sealed and heated in an oven at 180 °C for 12 hours to complete the reaction. After cooling to room temperature, the product was filtered using a Buchner funnel under vacuum, then washed with ethanol and DI water to remove residual reactants. The collected

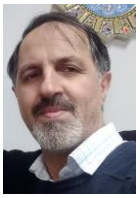

Dr. Reza Najjar, professor of chemistry currently working at the Faculty of Chemistry, University of Tabriz. Has has obtained PhD in polymer chemistry from Aachen University of Technology (RWTH-Aachen Germany) in June 2006, M. Sc., Chemistry, Sharif University of Technology, Tehran, Iran 1997, and B. Sc., Chemistry, University of Tabriz, Iran, 1994. His main research is focused on the preparation of new materials and investigation of their performance in various applications mainly related to the energy issues.

Reza Najjar, e-mail: najjar@tabriz.ac.ir T tel: +98-41-33393101, Cellphone: +98-912-0717158

precipitate was air-dried and further dried in a vacuum oven at 80 °C for 6 hours, yielding 1.32 g of product with an 86% yield.

2.3. Synthesis of P4VPy/NCS/PAni nanocomposite

Adequate amounts of the PAni, NCS and P4VPy were weighed into a mortar and mechanically blended to prepare a homogeneous P4VPy/NCS/PAni nanocomposites. The nanocomposites were then annealed at 80 °C for up to 25 h. The schematic representation of the detailed steps for preparation of the P4VPy/NCS/PAni nanocomposites are illustrated in Fig. 1. The relative weight ratios of P4VPy to NCS and PAni was varied and their effect on the performance of the nanocomposites was studied.

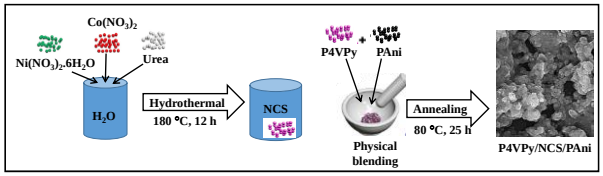

Fig. 1. the style to be used for graphs.

2.4. Characterizations

The SEM images and elemental analysis of the samples were obtained using a field emission scanning electron microscope (FE-SEM), specifically the Tescan MIRA3 FEG-SEM model from the Czech Republic, equipped with an energy dispersive X-ray spectroscopy (EDS) system. X-ray diffraction (XRD) patterns were recorded using a MAC Science M18XHFSRA instrument with CuKα radiation as the X-ray source. Fourier transform infrared (FT-IR) spectra were collected with a Perkin Elmer Spectrum One System spectrometer from the USA. The NCS samples underwent calcination in a tube furnace manufactured by Nabertherm, Germany.

2.5. Electrochemical measurements

An Origa Flex-OGF 01 A potentiostat-galvanostat electrochemical workstation (France), connected to a computer, was utilized to perform electrochemical measurements including electrochemical impedance spectroscopy (EIS), galvanostatic charge/discharge (GCD), and cyclic voltammetry (CV). The working electrode was prepared by coating the active electrode material onto a glassy carbon electrode. A platinum wire served as the counter electrode, and all measurements were conducted against an Ag/AgCl reference electrode. A 1 M H_2SO_4 solution was used as both the electrolyte and analysis medium. The active materials—P4VPy, P4VPy/NCS, and P4VPy/NCS/PAni—were each dispersed in N-methylformamide (NMF) and sonicated in an ultrasonic bath until a uniform slurry was formed. A suitable amount of this slurry was then evenly applied onto a cleaned glassy carbon electrode (0.4 cm diameter, approximately 0.126 cm² active area) to fabricate the working electrode, which was subsequently dried in an oven at 80 °C for around 4 hours.

The CV curves which were recorded at varying potential scan rates, and Eq. 1 were used to estimate the specific capacitance (C_{sp}) of the fabricated electrodes.

$$C_{sp} = \frac{1}{A \times v \times \Delta v} \int_{V_i}^{V_f} I dV \qquad \text{Eq. 1}$$

In Eq. 1, C_{sp} denotes the specific capacitance (F g^{-1}), I represents the current (A), A shows the active surface area of electrode (cm^2), $\boldsymbol{v}$ = scan rate (mV s^{-1}) and the observed potential window (V) is denoted with ΔV.

Also the GCD test results measured at varying constant current densities were utilized to estimate C_{sp} of electrodes by using Eq. 2.

$$C_{sp} = \frac{I \times \Delta t}{A \times \Delta v} \qquad \text{Eq. 2}$$

where I represents the constant current (A), Δt denotes discharging time (s), A is active area of electrode (cm^2), and ΔV represents the observed potential window (V).

3. Results and discussion

FT-IR spectra of P4VPy, P4VPy/NCS, and P4VPy/NCS/PAni are shown in Fig. 2. The addition of NCS nanoparticles to P4VPy introduces a strong absorption band around 664 cm^{-1}, related to NiS and CoS bonds. However, NCS nanoparticles do not cause disappearance or significant shifts in the polymer absorption bands, indicating no strong interactions between polymers and NCS. The main difference is the reduced relative intensity of polymer peaks due to the strong NCS bands.

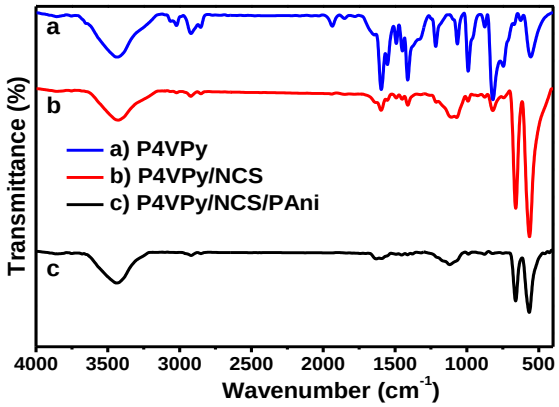

Fig. 2. The FT-IR spectra of: a) P4VPy, b) P4VPy/NCS and c) P4VPy/NCS/PAni samples measured as KBr disc.

The surface morphology of P4VPy/NCS/PAni sample was characterized via SEM micrographs and exhibited in Fig. 3. The SEM micrographs of the optimized P4VPy/NCS/PAni nanocomposite have revealed a very microporous structure for this sample.

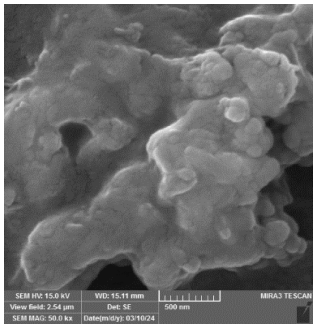

Fig. 3. SEM images of P4VPy/NCS/PAni nanocomposite with magnifications of 50 K.

The porous structure can significantly boost the specific capacitance (Csp) of the nanocomposite by enabling better electrolyte ion diffusion and providing a larger surface area for charge storage. EDX mapping (Fig. 4) confirmed uniform distribution of elements (C, N, O, Ni, Co, S) in the $NiCo_2S_4$ and P4VPy/NCS/PAni samples, indicating efficient mixing without noticeable agglomeration of NCS or PAni particles.

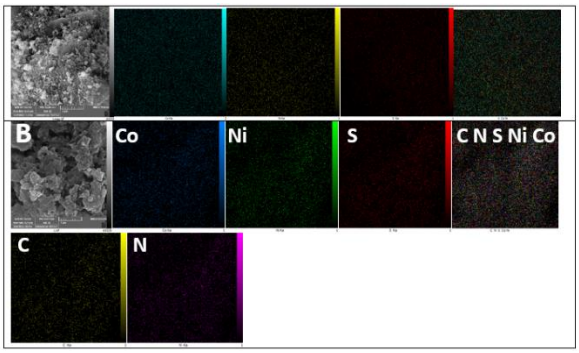

Fig. 4. The EDX mappings of the A) NiCo2S4 and B) P4VP/NCS/PAni nanocomposite samples.

The atomic ratio of Co to Ni in the P4VPy/NCS/PAni nanocomposite is 63.74% to 36.26%. Its flower-like morphology enhances charge transfer. The unique arrangement of benzene rings in PAni chains enables trapping of sulfide and oxide groups, leading to chain expansion and improved ion accessibility. Thus, PAni's structure promotes better interaction between electrolyte ions and active electrode sites compared to other electroactive materials.

3.2 Electrochemical investigations

CV curves of electrodes made with different materials were recorded between -0.4 V and 0.4 V at scan rates of 10, 30, 60, and 90 mV/s (Fig. 5). The curves show a quasi-rectangular, symmetrical shape, indicating fast, reversible Faradaic reactions and ideal capacitor behavior. Higher scan rates improve the rectangular shape, reflecting enhanced capacitive performance.

Table 1
The C_{sp} values calculated by using Eq. 1 from CV curves for electrodes prepared by using P4VPy, P4VPy/NCS and P4VPy/NCS/PAni at different potential scan rates in acidic media.

Electorde	C_s (F g^{-1}), Scan Rate (mV s^{-1})			
	10	30	60	90
P4VPy	184.08	132.44	107.28	94.53
$NiCo_2S_4$/P4VPy	350.39	240.03	192.38	172.24
PAni/$NiCo_2S_4$/P4VPy	482.22	362.20	295.24	261.76

3.3 GCD characteristics

The GCD performance of electrodes was evaluated at varying current densities (0.05–0.20 mA·cm^{-2}). As shown in Fig. 6, all electrodes demonstrated Faradaic behavior, with the P4VPy/NCS/PAni-based electrode exhibiting the longest discharge time. Specific capacitance (Csp) values, calculated from GCD data (Eq. 2, Table 2), decreased with increasing current density. At 0.20 mA·cm^{-2}, Csp values for P4VPy, P4VPy/NCS, and P4VPy/NCS/PAni were 18.33, 40.57, and 64.58 F·g^{-1}, respectively. The superior performance of P4VPy/NCS/PAni is attributed to its porous structure, which enhances ion diffusion and charge storage, as well as the synergistic effect of NCS and PAni that improves conductivity and promotes faster redox reactions.

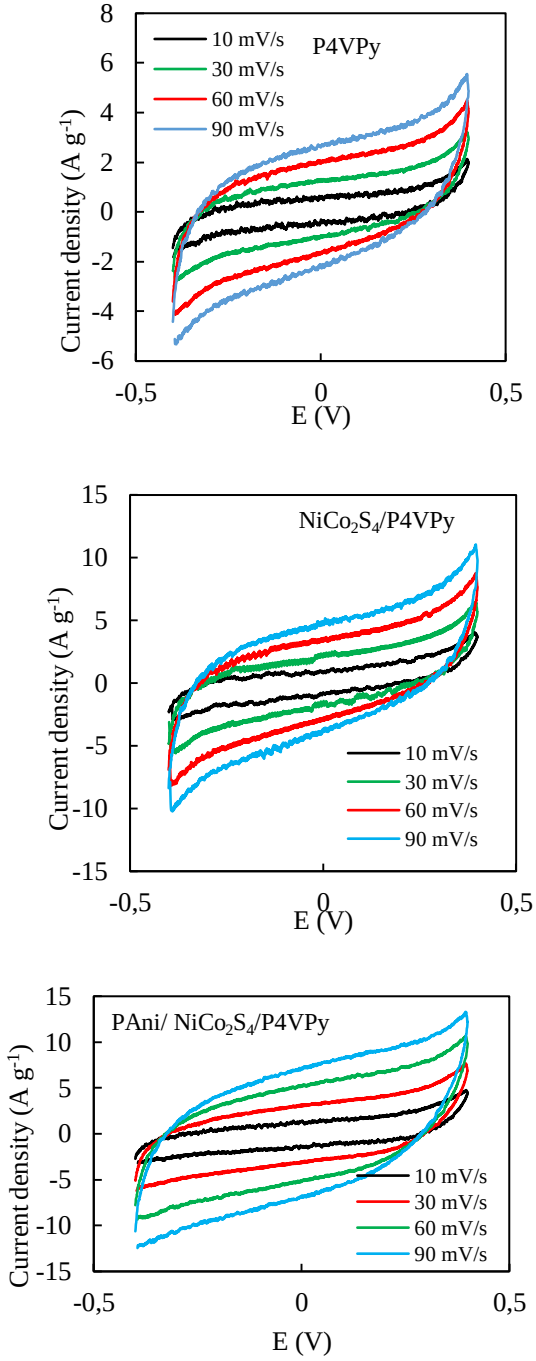

Fig. 5. CV curves for electrodes prepared by using A) P4VPy, B) P4VPy/NCS and C) P4VPy/NCS/PAni and measured at different potential scan rates in alkaline media.

Table 2
The C_{sp} values for electrodes prepared by using P4VPy, P4VPy/NCS, and P4VPy/NCS/PAni as electroactive materials, calculated via Eq. 2 and data extracted from GCD curves measured in different constant current densities in alkaline media.

. Electorde	C_s (F g^{-1}), Current (mA)			
	0.05	0.1	0.15	0.2
PVP	35.41	24.16	21.12	18.33
$NiCo_2S_4$/PVP	113.46	61.63	63.31	40.57
PA/ $NiCo_2S_4$/PVP	182.86	104.16	109.21	64.58

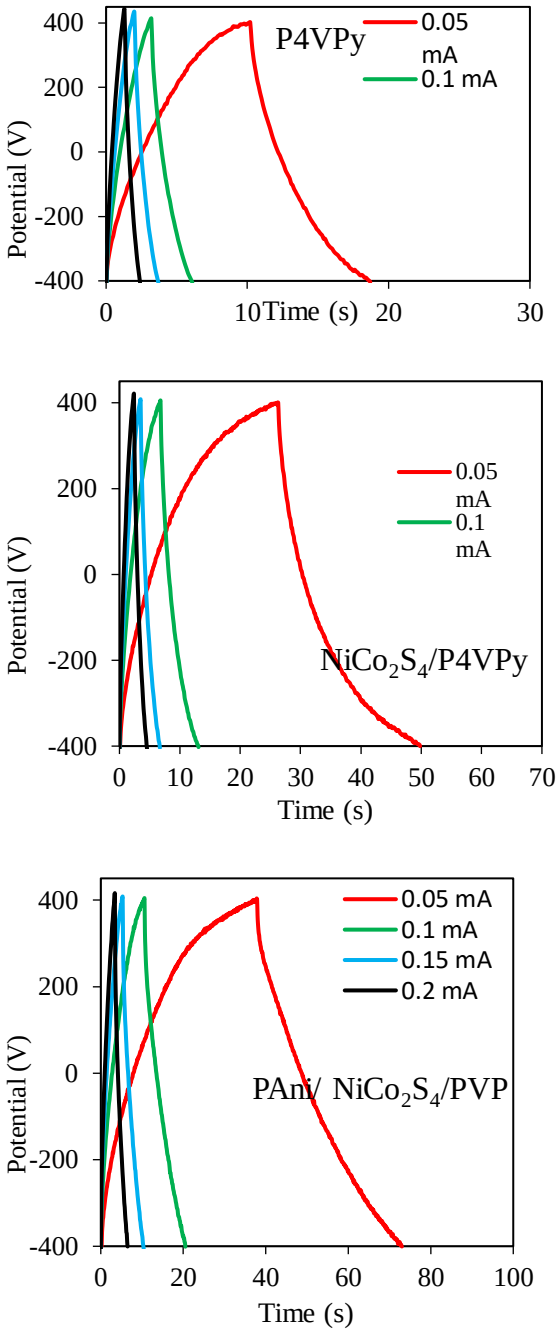

Fig. 6. GCD curves for A) P4VPy, B) P4VPy/NCS, C) P4VPy/NCS/PAni electrodes in different constant current densities in alkaline media

4- Conclusions

The PAni and NCS nanoparticles, synthesized via a simple hydrothermal method, were uniformly dispersed in the P4VPy matrix to form P4VPy/NCS/PAni nanocomposites. SEM and EDX analyses confirmed the homogeneous distribution of the mixed transition metal sulfide and conductive polymer nanoparticles. The synergistic effects of these components enhanced ionic conductivity by increasing the number of electroactive sites. This increase in active surface area provided additional pathways for efficient electron transfer and electrolyte ion diffusion, facilitating redox reactions. Ultimately, the optimized nanocomposite exhibited a maximum specific capacitance of 347.3 F/g at a scan rate of 90 mV/s and 95.82 F/g from GCD tests at 0.20 mA, demonstrating its potential as a high-performance electrode material for advanced supercapacitors.

Acknowledgement

The work was supported by the University of Tabriz which the Authors gratefully acknowledge.

References

[1] A. K. Das, S. Sahoo, P. Arunachalam, S. Zhang, and J.-J. Shim, *RSC Adv.*, 6 (2016) 107057–107064
[2] S. Prasad, D. Durairaj, M. AlSalhi, J. Theerthagiri, P. Arunachalam, and G. Durai, *Energies*, 11 (2018) 281
[3] R. R. Neiber *et al*, *J. Energy Storage*, P. Arunachalam, and G. Durai, *Energies*, 52 (2022) 104900
[4] M. D. Stoller, S. Park, Y. Zhu, J. An, and R. S. Ruoff, *Nano Lett*, 8 (2008) 3498–3502
[5] H. P. Wu *et al*, in *2010 8th International Vacuum Electron Sources Conference and Nanocarbon*, (2010) 465–466
[6] J. Theerthagiri *et al*, *J. Solid State Chem*, 267 (2018) 35–52
[7] S.-Y. Hsu, F.-H. Hsu, J.-L. Chen, Y.-S. Cheng, J.-M. Chen, and K.-T. Lu, *Mater. Chem*, 5 (2021) 4937–4949
[8] B. Gao *et al*, *J. Mater. Chem*, 7 (2009) 14–37
[9] M. Ahmad *et al*, *J. Power Sources*, 532 (2022) 231414
[10] B. Vedhanarayanan, K. C. S. Lakshmi, and T. W. Lin, *Batteries*, 9 (2023)
[11] M. G. Hosseini and E. Shahryari, *Ionics (Kiel)*, 25 (2019) 2383–2391
[12] N. Duraisamy *et al*, *J. Mater. Sci. Mater*, 30 (2019) 7435–7446
[13] V. Kumar and H. S. Panda, *Mater. Chem. Phys*, 272 (2021) 125042
[14] J. Park, S. Jo, N. Kitchamsetti, S. Zaman, and D. Kim, *J. Alloys Compd*, 926 (2022) 166815
[15] S. Bhadra and D. Khastgir, *Polym. Test*, 7 (2008) 851–857
[16] L. Zarei-Gharehbaba, R. Najjar, M. G. Hosseini, and P. YardaniSefidi, *Polym. Compos*, n/a (2024)